MCR-ALS–RESOLVED MULTI-EXCITATION HYPERSPECTRAL IMAGING FOR SPATIOTEMPORAL TRACKING OF DRUG RELEASE KINETICS

Kristina Ghahramanyan[1,†], *Fernando Villarruel*[1,†], *Ani Avetisyan*[1], *Ekaterina Baidiuk*[1], *and Narine Sarvazyan*[1,2]

[1]L. A. Orbeli Institute of Physiology, National Academy of Sciences of the Republic of Armenia, Yerevan, Armenia
[2]George Washington University, Washington, DC, United States
[†]These authors contributed equally to this work and share first authorship.

ABSTRACT

Collagen biomaterials are widely used as carriers for local drug delivery, where the release rate and the spatial spread of the drug determine its local concentration and the duration of treatment. Conventional release assays based on HPLC or UV–Vis spectrophotometry measure the total drug concentration in a surrounding liquid, but provide no information on how the released drug is distributed in the medium. This study uses multi-excitation hyperspectral imaging (ME-HSI) combined with multivariate curve resolution–alternating least squares (MCR-ALS) as a non-destructive method to map the spatial distribution of drugs and follow their release over time. Type I collagen sponges loaded with two fluorescent drugs, harmalol and ciprofloxacin, were placed on 0.75% agarose gel and imaged from 440 to 600 nm under six excitation wavelengths (310–400 nm) at eight time points over 55 h. Trilinear MCR-ALS decomposed the image series into two fluorescence components (99.2% explained variance, 6.84% lack of fit), whose excitation and emission maxima agreed with fluorescence spectroscopy of the drug mixture. Maps and radial profiles of the component scores showed how each drug diffused from the sponge into the gel over time. Harmalol was mostly released and reached the entire gel, whereas a large part of the ciprofloxacin remained in the sponge. Integrating the radial profiles at each time point followed the release of the two drugs independently, with linear release during the first hours ($R^2 = 0.992$ for harmalol and 0.954 for ciprofloxacin). These results show that ME-HSI with trilinear MCR-ALS can simultaneously track the spatial transport and release kinetics of more than one drug from a biomaterial.

Index Terms— *Multi-excitation hyperspectral imaging, fluorescence imaging, multivariate curve resolution, drug release, collagen biomaterials*

1. INTRODUCTION

Collagen is widely used as a carrier for local drug delivery in wound care. It is biocompatible and biodegradable, and as a porous sponge it can absorb a drug solution and release it directly at the wound site, providing a high local concentration with low systemic exposure [1]. Such carriers can also hold more than one drug, for example to combine treatments or to obtain a synergistic effect [2]. The release rate and the spread of each drug determine its local concentration and the duration of the treatment, and they depend on diffusion, solubility, and interactions between the drug and the matrix [3,4].

In a conventional release assay, the loaded material is kept in a liquid medium, and the drug concentration in this medium is measured at selected times by high-performance liquid chromatography (HPLC) or UV–Vis spectrophotometry [5,6]. These assays give the total amount of drug released over time, but provide no information on how the released drug is distributed. In tissue, the released drug spreads by diffusion, and its concentration changes with the distance from the carrier. This spatial information can be obtained by imaging the drug in a hydrogel such as agarose, which serves as a simple tissue model [7,8].

Many drugs are intrinsically fluorescent. For drugs that are not, a fluorescent surrogate molecule that diffuses and is released in a similar way can be used, or the drug itself can be labeled with a fluorescent marker. In all three cases, the release can be followed directly by fluorescence imaging. Hyperspectral imaging (HSI) records a full emission spectrum at each pixel and therefore provides both the location of a fluorescent compound and its spectral signature [9,10]. Multi-excitation HSI (ME-HSI) adds another dimension by recording the emission under several excitation wavelengths. Each fluorescent compound then contributes with its own pair of excitation and emission profiles, which makes it possible to distinguish several compounds within the same images [11].

The spectrum recorded at each pixel is the sum of the contributions of all fluorescent compounds present, and chemometric methods are needed to resolve these contributions. Multivariate curve resolution–alternating least squares (MCR-ALS) decomposes such data into the spectral profile of each component and its score at each pixel, which can be displayed as a distribution map [12,13]. For ME-HSI data, the images recorded under all excitation wavelengths are analyzed together with common emission profiles, and a trilinearity constraint requires the map of each component to have the same shape under every excitation wavelength, with an intensity that follows its excitation profile. The excitation profile, emission profile, and map of each component are thereby resolved together [11,14,15].

In this study, ME-HSI with trilinear MCR-ALS was used to follow the release of two fluorescent drugs, harmalol and ciprofloxacin, from type I collagen sponges into agarose gel over 55 h. The resolved maps were used to describe how each drug spread through the gel and left the sponge, and the

integrated scores were used to compare the release kinetics of the two drugs.

2. MATERIALS AND METHODS

2.1. Sample Preparation

Collagen sponges (n = 2) were prepared from type I collagen, which was extracted from bovine Achilles tendons with 0.5 M acetic acid, precipitated with sodium chloride, frozen, and lyophilized. Harmalol was purchased from Sigma-Aldrich (St. Louis, MO, USA). Ciprofloxacin, bought at a local pharmacy, was purified by high-speed centrifugation and filtration. The concentrations of the two drug solutions were adjusted so that both gave fluorescence signals of similar intensity, as measured by fluorescence spectroscopy, and the solutions were then mixed. The sponges were loaded by slowly adding 2 mL of the mixture and were left to dry for 24 h. After drying, they were placed in the middle of 90 mm Petri dishes on 10 mL of 0.75% (w/v) agarose gel [7].

2.2. ME-HSI Acquisition

The fluorescence was recorded by a Nuance FX hyperspectral camera (PerkinElmer/CRi, Waltham, MA, USA) through a Nikon AF Micro-Nikkor 60 mm f/2.8D lens. For excitation, six narrow-band LEDs (Mightex, Pleasanton, CA, USA; bandwidth of about 10 nm) were mounted 20 cm above the sample and switched on one at a time; their center wavelengths were 310, 325, 340, 365, 385, and 400 nm. Under each excitation wavelength, the emission was recorded from 440 to 600 nm in 10 nm steps (17 channels). Images were acquired at 0, 1, 2, 3, 4, 6, 30, and 55 h after placement on the gel. All measurements were performed in a darkroom, and the optical power of each LED was measured. Figure 1 summarizes the experimental workflow.

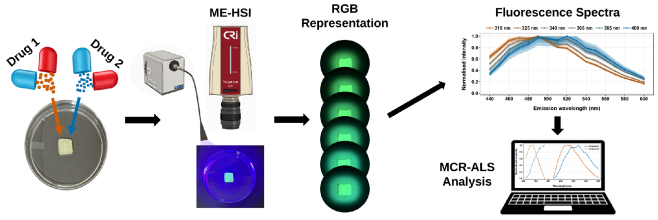


Figure 1. Overview of the study: a collagen sponge loaded with two drugs is placed on agarose gel and imaged by ME-HSI under six excitation wavelengths, and the corrected spectra are decomposed by MCR-ALS.

2.3. Fluorescence Spectroscopy

The excitation–emission matrix (EEM) of the drug mixture in solution was recorded with a FluoroMax Plus spectrofluorometer (HORIBA Jobin Yvon, Edison, NJ, USA). To allow a direct comparison with ME-HSI, the same excitation wavelengths and emission range as in Section 2.2 were used. The excitation and emission slit widths were 2 and 3 nm, respectively, and the spectra were corrected by the instrument software.

2.4. Data Preprocessing

The raw intensity of each pixel was divided by the spectral sensitivity of the camera, the exposure time, and the optical power of the LED to obtain the corrected fluorescence. Only pixels inside the dish were kept for analysis. The 90 mm dish spanned about 225 pixels, which gives a pixel size of about 0.4 mm. For comparison with the EEM measured in solution (Section 2.3), an EEM was also calculated from the images by averaging the corrected spectra over the sponge region.

2.5. MCR-ALS Analysis

The data from all excitation wavelengths and time points were arranged in a column-wise augmented matrix. Each excitation wavelength gave one data block, in which every row was the emission spectrum of one pixel at one time point and every column one emission wavelength, and the six blocks were then placed one below another. This matrix was decomposed by MCR-ALS with a trilinearity constraint on the augmented mode [14], which corresponds to the model

$$d(p, t; \lambda_{em}, \lambda_{ex}) = \sum_{k=1}^{K} m_k(p, t)\, a_k(\lambda_{ex})\, s_k(\lambda_{em}) + e \quad (1)$$

In (1), $d(p,t;\lambda_{em},\lambda_{ex})$ is the corrected fluorescence at pixel p and time t, K is the number of components, $m_k(p,t)$ is the score of component k, $a_k(\lambda_{ex})$ and $s_k(\lambda_{em})$ are its excitation and emission profiles, and e is the residual. The profiles were further constrained by non-negativity, and the emission profiles by unimodality. The model fit was evaluated by the explained variance and the lack of fit (LOF) [12], using the MCR-ALS GUI 2.0 in MATLAB [16].

2.6. Spatial and Kinetic Analysis

The scores $m_k(p,t)$ were refolded into a map of each component at each time point. In each map, a radial profile was taken from the sponge edge to the dish wall, over about 90 pixels (35 mm), and scaled to the maximum score of the component, so that the two drugs could be compared on the same relative scale. The harmalol maps contained a constant background that was already present at 0 h; this background was subtracted from the harmalol radial profiles and integrated scores. The integrated score of each drug in the gel was calculated as the area under its radial profile outside the sponge, in arbitrary units (a.u.), and a linear fit of the integrated score against time was used to describe the initial release. The scores are relative values, and drug concentrations were not calculated in this study.

3. RESULTS AND DISCUSSION

3.1. Fluorescence of the Two Drugs

Figure 2 shows the EEM of the sponge loaded with the drug mixture, calculated from the corrected ME-HSI images (Figure 2A), and the EEM of the drug mixture measured in solution by fluorescence spectroscopy (Figure 2B). Both

EEMs contain two fluorescence regions, one with its maximum at about 365/520 nm (exc/em) and the other at about 340/480–490 nm. Fluorescence spectroscopy is a highly sensitive technique and the standard method for characterizing fluorescent compounds [17], so the close agreement between the two EEMs confirms that the corrected images reproduce the fluorescence of the drugs.

The two regions correspond to the two drugs. Harmalol absorbs near 370 nm and emits at about 480 and 540 nm from its cationic and zwitterionic forms [18], so its emission covers the region excited at longer wavelengths and emitting near 520 nm. Ciprofloxacin has its excitation and emission maxima at about 320 and 450 nm [19] and therefore contributes mainly to the region excited at shorter wavelengths.

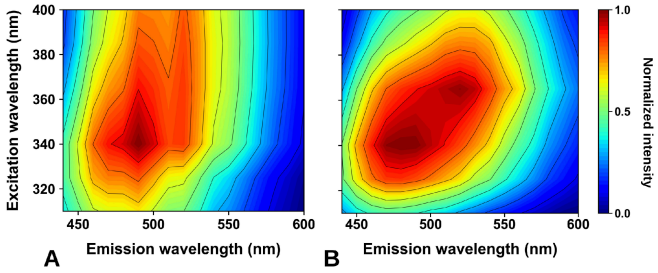


Figure 2. EEMs of (A) the collagen sponge loaded with the drug mixture, calculated from the corrected ME-HSI images, and (B) the drug mixture in solution, measured by fluorescence spectroscopy.

3.2. Resolution of the Two Drugs by MCR-ALS

Trilinear MCR-ALS resolved the image series into two components with 99.2% explained variance and a LOF of 6.84%. Figure 3 (left) shows their excitation and emission profiles. The profile in Figure 3A, with its maximum at 365/530 nm, corresponds to harmalol, and the profile in Figure 3B, with its maximum at 340/470 nm, corresponds to ciprofloxacin. Both maxima agree with the two regions of the EEMs in Figure 2.

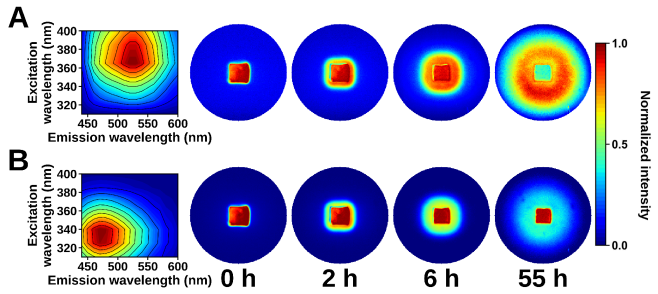


Figure 3. Excitation–emission profiles (left) and score maps at 0, 2, 6, and 55 h (right) of (A) harmalol and (B) ciprofloxacin resolved by MCR-ALS.

Figure 3 (right) shows the corresponding score maps at 0, 2, 6, and 55 h. At 0 h, the signal of both drugs was almost entirely confined to the sponge. After 2 h, each drug formed a narrow zone in the gel around the sponge, and by 6 h the harmalol zone was wider and more intense than the ciprofloxacin zone. At 55 h, harmalol covered the entire gel up to the dish wall, with the highest scores in a ring around the sponge and lower scores in the sponge itself. Ciprofloxacin covered most of the gel, but its highest scores remained in the sponge, and its signal decreased gradually toward the dish wall.

Figure 4 shows radial profiles of the normalized scores, taken along a line from the sponge edge to the dish wall at every time point. These profiles describe how the score of each drug changes with the distance from the sponge and how this distribution develops over time.

During the first 6 h, harmalol moved steadily away from the sponge (Figure 4A), and by 30 h it had almost reached the dish wall. At 30 and 55 h, its signal close to the sponge was lower than further out in the gel. This shows that the release had stopped while the harmalol already in the gel continued to diffuse outward, and that most of the drug had been released by this time.

Ciprofloxacin spread into the gel more slowly than harmalol (Figure 4B), and its release stopped much earlier, at about 6 h. After this time, its signal near the sponge decreased as the drug already in the gel diffused outward [3]. In contrast to harmalol, the highest ciprofloxacin signal remained in the sponge throughout the experiment, showing that a large part of the drug was retained inside the material. We attribute this mainly to the aqueous solubility of ciprofloxacin, which is lowest near neutral pH, where the molecule exists as a zwitterion [20]. When the loaded sponge was dried, part of the ciprofloxacin may have precipitated within the collagen matrix, so that only the fraction that redissolved in the water taken up from the gel could be released. Harmalol is almost completely protonated at neutral pH [18], which favors its solubility and allows it to diffuse out of the sponge.

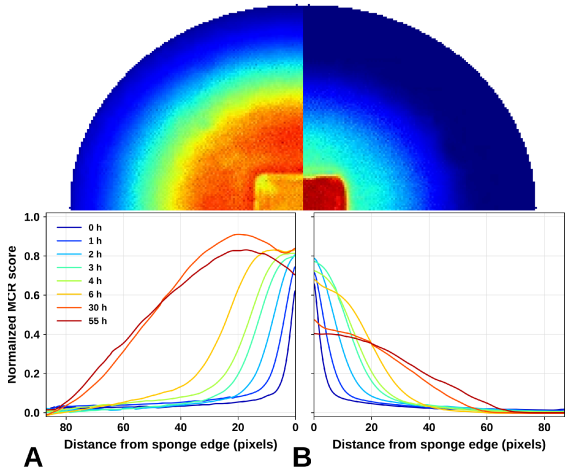


Figure 4. Score maps of harmalol (left) and ciprofloxacin (right) at 30 h (top), and radial profiles of (A) harmalol and (B) ciprofloxacin from the sponge edge to the dish wall at all time points (bottom).

3.3. Release Kinetics

Figure 5 shows the integrated scores of the two drugs, calculated as the area under the radial profiles in Figure 4. These scores reflect the relative amount of each drug in the gel over time. During the first hours, both drugs were released at a constant rate, with linear fits over 0–6 h for harmalol ($R^2 = 0.992$) and over 0–4 h for ciprofloxacin ($R^2 = 0.954$).

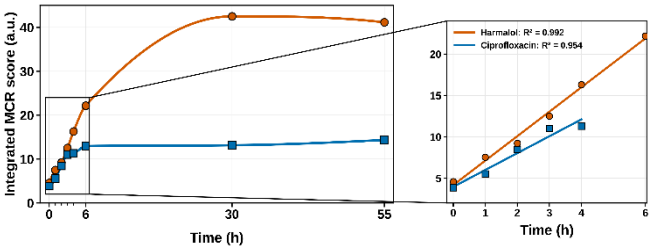


Figure 5. Integrated scores (area under the radial profiles) of harmalol and ciprofloxacin over 55 h (left) and linear fits of the initial release (right).

The two drugs differed in both the rate and the duration of their release. During the first hours, the harmalol curve had a steeper slope than the ciprofloxacin curve, in agreement with the faster spread of harmalol in the gel. The release of ciprofloxacin reached a plateau at about 6 h, whereas harmalol continued to be released after 6 h and reached a plateau by 30 h. Harmalol was therefore released both faster and for a longer time than ciprofloxacin.

The integrated scores describe the release in relative terms. In future studies, calibrating the scores with known drug concentrations will allow each pixel to be converted into a concentration and these values to be summed over the sponge and the gel, so that the released percentage of each drug can be calculated at every time point.

4. CONCLUSION

This study shows that ME-HSI combined with trilinear MCR-ALS can map the release of more than one drug from a collagen biomaterial into a tissue model. From a single image series, the fluorescence of harmalol and ciprofloxacin was resolved into two components that agreed with fluorescence spectroscopy of the drug mixture, and a separate map of each drug was obtained at every time point. Both drugs were released at a constant rate during the first hours. Harmalol was released faster and for a longer time, and its release reached a plateau by 30 h; most of it left the sponge and spread across the entire gel. Ciprofloxacin release stopped at about 6 h, and a large part of the drug remained in the sponge. Such spatially resolved information on each drug is not available from conventional release assays. Future work will include calibration with known drug concentrations to express the release as a percentage of the loaded amount, sponges loaded with a single drug, and more time points between 1 and 30 h. The approach can also be extended to non-fluorescent drugs by using fluorescent surrogates or labels.

5. ACKNOWLEDGMENT

This work was supported by the European Union ERA CHAIR award (NAS-SAR 101087403) and the Republic of Armenia HESC (24PostDoc/2-2G002) grants.

6. REFERENCES

[1] Z. Ruszczak and W. Friess, “Collagen as a carrier for on-site delivery of antibacterial drugs,” *Adv. Drug Deliv. Rev.*, vol. 55, no. 12, pp. 1679–1698, 2003.

[2] D. Simões, S. P. Miguel, M. P. Ribeiro, P. Coutinho, A. G. Mendonça, and I. J. Correia, “Recent advances on antimicrobial wound dressing: A review,” *Eur. J. Pharm. Biopharm.*, vol. 127, pp. 130–141, 2018.

[3] J. Siepmann and F. Siepmann, “Modeling of diffusion controlled drug delivery,” *J. Control. Release*, vol. 161, no. 2, pp. 351–362, 2012.

[4] M. P. Singh, J. A. Lumpkin, and J. Rosenblatt, “Effect of electrostatic interactions on polylysine release rates from collagen matrices and comparison with model predictions,” *J. Control. Release*, vol. 35, nos. 2–3, pp. 165–179, 1995.

[5] S. D’Souza, “A review of in vitro drug release test methods for nano-sized dosage forms,” *Adv. Pharm.*, vol. 2014, Art. no. 304757, 2014.

[6] Q. Wang, G. Wang, S. Xie, X. Zhao, and Y. Zhang, “Comparison of high-performance liquid chromatography and ultraviolet-visible spectrophotometry to determine the best method to assess levofloxacin released from mesoporous silica microspheres/nano-hydroxyapatite composite scaffolds,” *Exp. Ther. Med.*, vol. 17, no. 4, pp. 2694–2702, 2019.

[7] F. Ye, S. W. Larsen, A. Yaghmur, H. Jensen, C. Larsen, and J. Østergaard, “Drug release into hydrogel-based subcutaneous surrogates studied by UV imaging,” *J. Pharm. Biomed. Anal.*, vol. 71, pp. 27–34, 2012.

[8] J. Østergaard, “UV imaging in pharmaceutical analysis,” *J. Pharm. Biomed. Anal.*, vol. 147, pp. 140–148, 2018.

[9] J. M. Amigo, “Practical issues of hyperspectral imaging analysis of solid dosage forms,” *Anal. Bioanal. Chem.*, vol. 398, no. 1, pp. 93–109, 2010.

[10] M. I. Sanhueza et al., “Confocal laser scanning microscopy as a novel tool of hyperspectral imaging for the localization and quantification of fluorescent active principles in pharmaceutical solid dosage forms,” *Microchem. J.*, vol. 168, Art. no. 106479, 2021.

[11] M. Ghaffari, A.-L. Chateigner-Boutin, F. Guillon, M.-F. Devaux, H. Abdollahi, and L. Duponchel, “Multi-excitation hyperspectral autofluorescence imaging for the exploration of biological samples,” *Anal. Chim. Acta*, vol. 1062, pp. 47–59, 2019.

[12] A. de Juan and R. Tauler, “Multivariate curve resolution: 50 years addressing the mixture analysis problem – A review,” *Anal. Chim. Acta*, vol. 1145, pp. 59–78, 2021.

[13] S. Piqueras, L. Duponchel, R. Tauler, and A. de Juan, “Resolution and segmentation of hyperspectral biomedical images by multivariate curve resolution-alternating least squares,” *Anal. Chim. Acta*, vol. 705, nos. 1–2, pp. 182–192, 2011.

[14] R. Tauler, I. Marqués, and E. Casassas, “Multivariate curve resolution applied to three-way trilinear data: Study of a spectrofluorimetric acid–base titration of salicylic acid at three excitation wavelengths,” *J. Chemometrics*, vol. 12, no. 1, pp. 55–75, 1998.

[15] R. Bro, “PARAFAC. Tutorial and applications,” *Chemom. Intell. Lab. Syst.*, vol. 38, no. 2, pp. 149–171, 1997.

[16] J. Jaumot, A. de Juan, and R. Tauler, “MCR-ALS GUI 2.0: New features and applications,” *Chemom. Intell. Lab. Syst.*, vol. 140, pp. 1–12, 2015.

[17] J. R. Lakowicz, *Principles of Fluorescence Spectroscopy*, 3rd ed. New York, NY, USA: Springer, 2006.

[18] M. P. Denofrio et al., “Photosensitizing properties and subcellular localisation of 3,4-dihydro-β-carbolines harmaline and harmalol,” *Photochem. Photobiol. Sci.*, vol. 22, no. 3, pp. 487–501, 2023.

[19] N. T. Barakat, A. M. El-Brashy, and M. E. Fathy, “Eco-friendly, sensitive and inventive first derivative synchronous spectrofluorimetric determination of ciprofloxacin and phenylephrine in their pure form, single and combined eye drops,” *BMC Chem.*, vol. 18, Art. no. 27, 2024.

[20] D. L. Ross and C. M. Riley, “Aqueous solubilities of some variously substituted quinolone antimicrobials,” *Int. J. Pharm.*, vol. 63, no. 3, pp. 237–250, 1990.